




Constraining the Earth-mass Primordial Black Hole Mergers Model of the Non-repeating FRBs Using the First CHIME/FRB Catalog

Min Meng, Qiu-Ju Huang, and Can-Min Deng 

Guangxi Key Laboratory for Relativistic Astrophysics, School of Physical Science and Technology, Guangxi University, Nanning 530004, China; dengcm@gxu.edu.cn

Received 2024 May 30; revised 2024 July 27; accepted 2024 August 13; published 2024 September 9

Abstract

In this paper, we upgrade the constraints for the Earth-mass primordial black hole mergers model based on the first Canadian Hydrogen Intensity Mapping Experiment (CHIME)/fast radio burst (FRB) catalog. Assuming the null hypothesis that the observed non-repeating FRBs originate from Earth-mass primordial black hole mergers, we find that how the charges were distributed in the primordial black hole population is well described by a double power-law function with typical charge value of $q_c/10^{-5} = 1.60^{+0.28}_{-0.28}$, where the power-law index $\alpha_1 = 2.33^{+0.15}_{-0.18}$ for $q < q_c$ and $\alpha_2 = 4.56^{+0.30}_{-0.26}$ for $q \geq q_c$. Here, q represents the charge of the black hole in units of \sqrt{GM} , where M is the mass of the black hole. Furthermore, we infer the local event rate of the bursts is $8.8^{+5.7}_{-2.1} \times 10^4 \text{ Gpc}^{-3} \text{ yr}^{-1}$, which indicates that an abundance of the primordial black hole population $f \gtrsim 10^{-4}$ is needed to account for the observed FRBs by CHIME. The results of this paper lay the basis for further research on the electromagnetic radiation background generated by the merger of primordial black hole mergers.

Key words: black hole physics – (stars:) gamma-ray burst: general – (cosmology:) dark matter

1. Introduction

Fast radio bursts (FRBs) are enigmatic astronomical radio transients with observed durations around a millisecond (Lorimer et al. 2007; Cordes & Chatterjee 2019; Petroff et al. 2019). To date, several hundred FRBs have been reported, the majority of which are one-off events, with only dozens of sources identified as repeaters (Cordes & Chatterjee 2019; Petroff et al. 2019; Zhang 2020a, 2023; Xiao et al. 2021). Some studies suggest that the non-repeaters might be intrinsically different from the repeaters (Palaniswamy et al. 2018; Cui et al. 2021; Zhong et al. 2022; Luo et al. 2023; Zhu-Ge et al. 2023). Recently, it is widely believed that repeating FRBs originate from magnetar activity (Popov & Postnov 2013; Kulkarni et al. 2014; Lyubarsky 2014; Katz 2016; Beloborodov 2017, 2020; Kumar et al. 2017; Metzger et al. 2017, 2019; Wadiasingh & Timokhin 2019; Lu et al. 2020; Lyu et al. 2021) or interactions in binary systems containing at least one compact object (Geng & Huang 2015; Dai et al. 2016; Gu et al. 2016, 2020; Dai 2020; Dai & Zhong 2020; Geng et al. 2020; Ioka & Zhang 2020; Zhang 2020b; Decoene et al. 2021; Deng et al. 2021; Kuerban et al. 2021; Wang et al. 2022; Lan et al. 2023). Due to the very limited observational information on non-repeating bursts, the question of their origin remains mysterious. Although non-repeating FRBs may originate from astrophysical processes such as the collapse of neutron stars into black holes (Falcke & Rezzolla 2014; Zhang 2014; Punsly & Bini 2016) or mergers of two compact stars (Kashiyama et al. 2013; Totani 2013; Mingarelli et al. 2015; Liu et al. 2016; Wang et al. 2016; Zhang 2016; Li et al.

2018; Liu 2018), it is very difficult to explain their extremely high event rates (Deng et al. 2019; Ravi 2019; Meng & Deng 2024). Given that existing astrophysical models do not perfectly explain non-repeating FRBs, alternative ideas have been proposed. These include oscillations or decay of superconducting cosmic strings (Vachaspati 2008; Cai et al. 2012a, 2012b; Yu et al. 2014; Zadorozhna 2015; Brandenberger et al. 2017; Ye et al. 2017; Cao & Yu 2018; Imtiaz et al. 2020) and our charged primordial black hole merger model (Deng et al. 2018). According to Deng (2021), mergers of the Earth-mass primordial black holes could serve as sources for non-repeating FRBs, potentially explaining all key observational features, particularly the high event rate.

In Deng (2021), we used the inchoate FRB samples to constrain the charged Earth-mass primordial black hole merger model. A power law distribution of the charges with a typical charge value $q_c = 1.59^{+0.08}_{-0.18} \times 10^{-5}$ is required to explain the data (Deng 2021). These charges may come from the process of accretion of magnetic monopoles in the early Universe (Deng et al. 2018; Wang & Deng 2024). Now a large and uniform FRB sample from the Canadian Hydrogen Intensity Mapping Experiment (CHIME) has been released. In this work, we use the first FRB catalog of CHIME to perform an updated constraint to our model.

2. Sample Selection

In this work, our analyses are based on the large uniform sample from the first CHIME/FRB catalog, which contains

474 non-repeating sources (CHIME/FRB Collaboration et al. 2021). In order to minimize the impact of selection effect, we need to weed out some bursts by following previous studies (CHIME/FRB Collaboration et al. 2021; Hashimoto et al. 2022; Qiang et al. 2022; Shin et al. 2023): (1) Bursts labeled with “excluded-flag = 1”, because they are detected either during pre-commissioning, epochs of low-sensitivity, or on days with software upgrades; (2) Bursts with signal-to-noise ratio (SNR) < 12, to exclude events that might lead to misclassification of FRBs and noise due to perceived differences in visual and system pipeline detection; (3) Bursts with $DM < 1.5 \max(DM_{\text{NE2001}}, DM_{\text{YMW16}})$, to ensure that the events come from cosmological distances. After all of the above exclusion criteria are applied, 281 non-repeating bursts remain which is the sample used for our analyses.

For those FRBs that did not have redshift measurements, we infer their redshifts from the extragalactic dispersion measures (DMs). Since the host galaxy’s contribution to DM is expected to be small in our model, the host galaxy DM is ignored.¹ Then, the observed DM can be divided into

$$DM = DM_{\text{MW}} + DM_{\text{IGM}}, \quad (1)$$

where DM_{MW} is the contribution from the disk and the halo of Milky Way. We infer the DM from the disk using the electron density model of Yao et al. (2017), and a fixed value of 30 pc cm^{-3} for the DM from the Milky Way halo is adopted. The DM_{IGM} is the contribution from the intergalactic medium, which is calculated as (Deng & Zhang 2014)

$$DM_{\text{IGM}}(z) = \frac{3cH_0\Omega_b f_{\text{IGM}} f_e}{8\pi G m_p} \int_0^z \frac{1+z'}{E(z')} dz', \quad (2)$$

where $\Omega_b = 0.0486$, $f_{\text{IGM}} = 0.83$, $f_e = 7/8$, and $H_0 = 67.74$ are the cosmological parameters. $E(z) = H(z)/H_0$ is the dimensionless Hubble parameter (Planck Collaboration et al. 2016), and m_p is the mass of a proton. When the value of DM subtracts the contribution from the Milky Way, the redshift z can be estimated from the above equation.

Following Deng (2021), and studies on gamma-ray bursts (Bloom et al. 2001; Sun et al. 2015; Zhang 2019), we estimate the isotropic energy of the FRBs within a uniform bandwidth of (ν_1, ν_2) in the burst-frame by

$$E = \frac{4\pi D_L^2}{1+z} F_\nu \int_{\nu_1/(1+z)}^{\nu_2/(1+z)} \left(\frac{\nu}{\nu_c} \right)^{-\gamma} d\nu, \quad (3)$$

where F_ν is the specific fluence, D_L is luminosity distance for a given redshift, γ is the spectral index of FRBs, and $\nu_c = 0.6 \text{ GHz}$ is the typical central frequency of CHIME. In this work, we adopt $\gamma = 1.6$ as in Deng (2021). $\nu_1 = 0.4 \text{ GHz}$ and $\nu_2 = 0.8 \text{ GHz}$ are adopted to uniformly correct the energy to the uniform band in the burst-frame.

¹ Nevertheless, we have examined the case for taking a relatively large DM value for the host galaxy, and we found that this did not significantly affect our results.

3. The Method and Results

The model of charged primordial black hole mergers for the non-repeating FRBs had been presented by Deng et al. (2018), Deng (2021) in detail. In the context of this model, the peak frequency of the radio bursts is related to the mass of the black holes as $\nu_p \sim (M/10^{-5} M_\odot)^{-1} \text{ GHz}$, and the energy of the bursts is $E \sim q^2 M c^2 \sim 10^{38} (q/10^{-6})^2 \nu_{p, \text{GHz}}^{-1} \text{ erg}$. Here, q is the charge of the primordial black holes in unit of \sqrt{GM} as defined in Deng et al. (2018). As in Deng et al. (2018), Deng (2021), we assume that the charges held by the primordial black holes satisfy an undetermined distribution of $\phi(q)$ for the whole population of primordial black holes.

Since no information is theoretically given about the form of $\phi(q)$, we simply do not know what the intrinsic distribution of q looks like. Therefore, it would be great if the intrinsic distribution of q , i.e., $\phi(q)$, can be derived in a non-parametric way. As we have done in the previous works (Deng et al. 2018; Deng 2021), we will use the non-parametric method developed by Sun et al. (2015) to derive the intrinsic form of $\phi(q)$. This method requires the assumption of the redshift distribution of the sources. For our model, the redshift distribution of the sources is theoretically predicted (see Equation (6)), so applying this method to our problem is self-consistent. Let us briefly review this method below.

For a radio telescope survey with fluence threshold of F_{th} , field of view Ω , and operational time T , the observed number of FRBs within the range of $(q, q+dq)$ is estimated as (Deng et al. 2018; Deng 2021)

$$dN = \frac{\Omega T}{4\pi} \phi(q) dq \int_0^{z_{\text{max}}(q)} \frac{n(z)}{1+z} \frac{dV(z)}{dz} dz, \quad (4)$$

where $V(z)$ is comoving volume, and $q \simeq 10^{-6} (E/10^{38} \text{ erg})^{1/2}$ is the charge value which is needed to account for the energy of the burst (Deng 2021). Also, $z_{\text{max}}(q)$ represents the maximum redshift where the FRBs can be detected by a radio telescope with fluence threshold of F_{th} . It is calculated by

$$F_{\text{th}} = \frac{(1+z_{\text{max}}) q^2 M c^2}{4\pi D_L^2}, \quad (5)$$

where $F_{\text{th}} = 0.4 \text{ Jy ms}$ is adopted in this work.² In the context of our model, the cosmic rate of the sources follows the primordial black hole binary merger rate, which is given by (Ali-Haïmoud et al. 2017; Deng 2021)

$$n(z) = n_0 (1+z)^3 (t_0/t_z)^{34/37}, \quad (6)$$

where t_0 is the age of the Universe at present, and $t_z = \int_z^\infty [(1+z')H(z')]^{-1} dz'$ the age of the Universe at a given redshift z . The local merger rate n_0 is calculated as

² A larger threshold does not affect our results significantly.

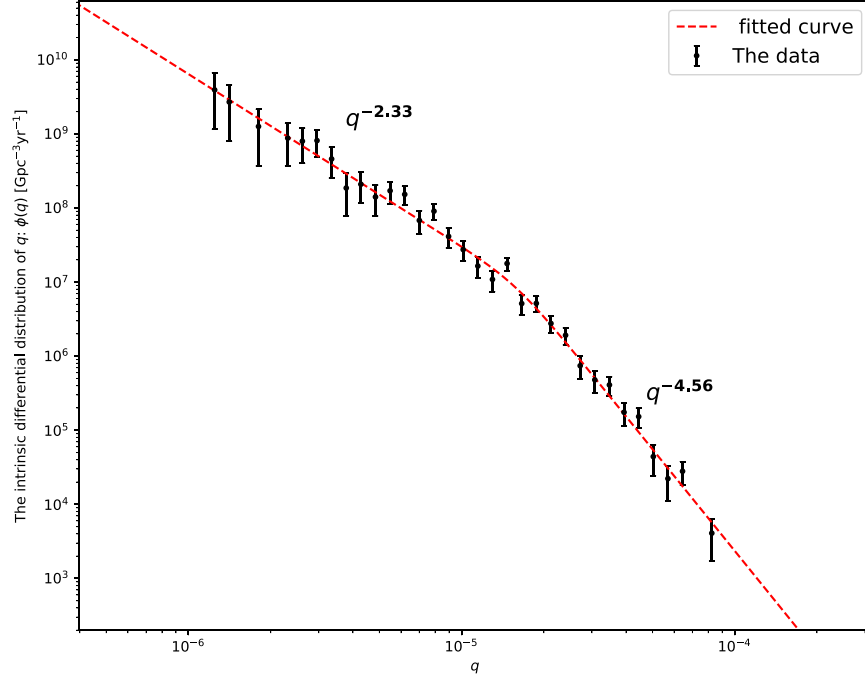


Figure 1. The intrinsic differential distribution of q is derived by using Equation (8) from the data directly, and the error bars represent the Poisson error. The best fit to the data is also shown.

follows (Ali-Haimoud et al. 2017; Deng 2021)

$$n_0 \simeq 10^{-3} \frac{\rho_0}{M_\odot t_0} m^{-32/37} f^2 (f^2 + \sigma_{\text{eq}}^2)^{-21/74}, \quad (7)$$

where $m = M/M_\odot$ is the dimensionless mass of primordial black holes, ρ_0 is the density of the matter in present Universe, f represents the proportion of primordial black holes to the matter of the Universe. and $\sigma_{\text{eq}} = 5 \times 10^{-3}$ is adopted for calculation (Deng 2021).

Since the CHIME/FRB sample is large enough, it allows us to make differential distributions and derive the intrinsic differential distribution of q from the observed data directly. Suppose that ΔN events are detected in a finite bin of q , then from q to $q + \Delta q$, one has (Sun et al. 2015)

$$\phi(q) \propto n_{0,q} \approx \frac{4\pi}{\Omega T} \frac{1}{f(q)} \frac{\Delta N}{\Delta q}, \quad (8)$$

and

$$f(q) = \int_0^{z_{\text{max}}(q)} (1+z)^2 \left(\frac{t_0}{t_z} \right)^{34/37} \frac{dV(z)}{dz} dz. \quad (9)$$

The result is shown in Figure 1. It is important to note that the black data points in Figure 1 are directly calculated from Equation (8) and represent the intrinsic distribution of q , not the observed distribution. As one can see, $\phi(q)$ exhibits the characteristics of a broken power law. To describe $\phi(q)$ analytically, we use a smooth broken power law function to fit

it. The form of the function is taken as (Sun et al. 2015)

$$\phi(q) \propto \left[\left(\frac{q}{q_c} \right)^{\omega\alpha_1} + \left(\frac{q}{q_c} \right)^{\omega\alpha_2} \right]^{-1/\omega}. \quad (10)$$

Accordingly, α_1 and α_2 are the power-law indices, and q_c represents the break charge of the distribution. ω defines the sharpness of the break, and $\omega = 3$ is adopted in this work. Using the Markov Chain Monte Carlo (MCMC) method as in Deng (2021), we get the posterior probability distribution of the model parameters: $q_c/10^{-5} = 1.60_{-0.28}^{+0.28}$, $\alpha_1 = 2.33_{-0.18}^{+0.15}$, and $\alpha_2 = 4.56_{-0.26}^{+0.30}$, in a 1σ confidence level. The fitting results are also displayed in Figures 1 and 2.

Furthermore, based on Equation (8), one can calculate the local event rate $n_{0,>q}$ as a function of q point by point,

$$n_{0,>q_i} \approx \frac{4\pi}{\Omega T} \sum_{q_i}^{q_{\text{max}}} \frac{1}{f(q_i)}, \quad (11)$$

where q_{max} is the maximum value in the sample of q . Then one can obtain the local event rate above q_{min} ,

$$n_0 \equiv n_{0,>q_{\text{min}}} \simeq 8.8_{-2.1}^{+5.7} \times 10^4 \text{ Gpc}^{-3} \text{ yr}^{-1}, \quad (12)$$

where $q_{\text{min}} = 1.2 \times 10^{-6}$ is the minimum value in the sample of q . Here the field of view of CHIME $\Omega/4\pi = 0.3\%$ and the survey time $T = 214.8$ days have been used for calculation (CHIME/FRB Collaboration et al. 2021).

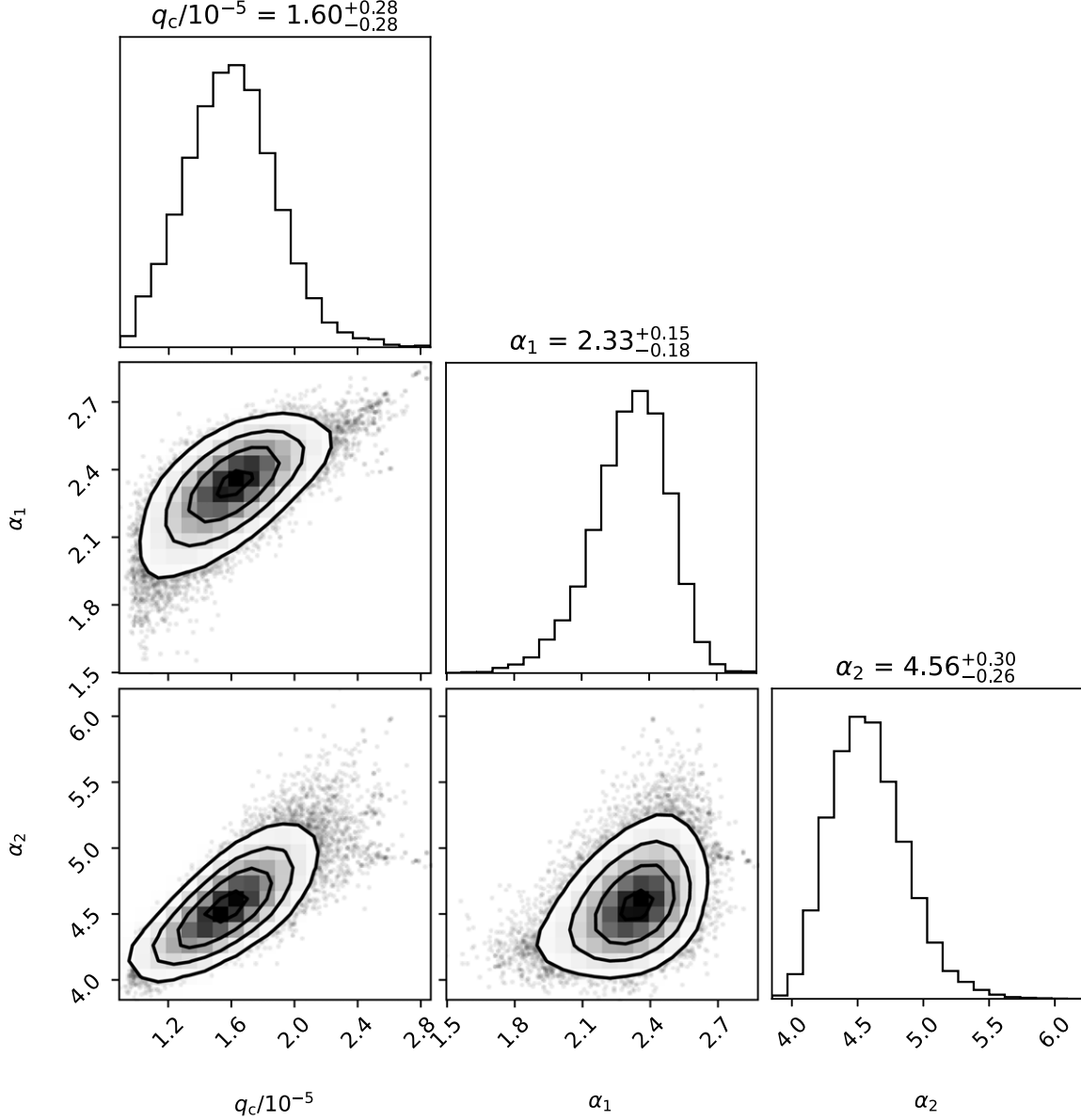


Figure 2. The posterior probability distribution of the fitting parameters derived by applying the MCMC method.

Going back to Equation (7), one then can infer that $f \gtrsim 10^{-4}$ is required to explain the observed number of bursts of the CHIME/FRB sample. Compared to the previous results in Deng (2021), one sees that the inferred values for $n_{0, > q_{\min}}$ are an order of magnitude larger. Moreover, a completely different power exponent is obtained in this work, where it is found that the distribution of q can only be described by a double power-law function, rather than by a simple power-law function in Deng (2021). The reason for these differences could be that different samples are used.

The results presented above are obtained by using the non-parametric method from the observed energy of the

FRBs directly, which focuses primarily on the intrinsic distribution of q , i.e., $\phi(q)$. In principle, the model should also account for the observed redshifts of the sample, and it would also provide constraints on $\phi(q)$. To do this, it is necessary to use the method of parameter fitting by assuming a specific form for $\phi(q)$, so we let this content appear in the Appendix.

4. Conclusions

In this work, we upgrade the constraints for the Earth-mass primordial black hole merger model based on the first CHIME/

FRB catalog. In the context of this model, we derived the charge distribution $\phi(q)$ in the primordial black hole population directly from the data by using a non-parametric method. We find that the $\phi(q)$ is well described by a double power-law function with typical charge value of $q_c/10^{-5} = 1.60^{+0.28}_{-0.28}$, where the power-law index $\alpha = 2.33^{+0.15}_{-0.18}$ for $q < q_c$ and $\beta = 4.56^{+0.30}_{-0.26}$ for $q \geq q_c$. Furthermore, we infer the local event rate of the bursts is $8.8^{+5.7}_{-2.1} \times 10^4 \text{ Gpc}^{-3} \text{ yr}^{-1}$, which indicates that an abundance of the primordial black hole populations $f \gtrsim 10^{-4}$ is needed to account for the observed FRBs by CHIME.

In principle, the primordial black holes could be charged stably by accretion magnetic monopoles (Wang & Deng 2024), which could result in a charge value up to $q \sim 10^{-4}$ (Deng et al. 2018). This also explains the energy of FRBs comfortably. If this is the case, then a natural inference arises that these charged primordial black holes must have produced a corresponding electromagnetic background when they orbit or merge with each other. This topic will be presented in another paper, based on the results of this work.

Acknowledgments

This work is supported by the National Natural Science Foundation of China (NSFC, Grant No. 12203013) and the Guangxi Science Foundation (grant Nos. 2023GXNSFBA026030 and Guike AD22035171).

Appendix

Similar to Equation (4), the theoretically observed number of sources in the redshift range of $(0, z_i)$ can be calculated as (Cao et al. 2018)

$$N(< z_i) = \frac{\Omega T}{4\pi} \int_0^{z_i} \frac{n(z)}{1+z} \frac{dV(z)}{dz} dz \int_{\max[q_{\text{th}}(z), q_{\text{min}}]}^{q_{\text{max}}} \phi(q) dq, \quad (\text{A1})$$

where $q_{\text{th}}(z)$ is the minimum q where the FRBs at z can be detected by a radio telescope with fluence threshold of F_{th} , and it can be calculated according to Equation (5).

To fit the observed redshift distribution, a specific function form of $\phi(q)$ is needed. As prior knowledge, we have derived $\phi(q)$ non-parametrically in the main text and found that it can be described well by Equation (10). Therefore, we adopt Equation (10) as $\phi(q)$ into Equation (A1) to perform model fitting. The fitting results are shown in Figures 3 and 4. It can be seen that the parameters of $\phi(q)$ obtained by fitting the observed redshift distribution here are in good agreement with those obtained in the main text, especially for α_1 and α_2 . However, the fitting value for the local event rate is $n_0 \simeq 4.89^{+0.31}_{-0.26} \times 10^5 \text{ Gpc}^{-3} \text{ yr}^{-1}$, which is larger than the value obtained in the main text by a factor of 3 within the error bar. We believe that this difference may be due to differences in methods. In this paper, we tend to adopt the results obtained in the main text because they are derived directly from the data

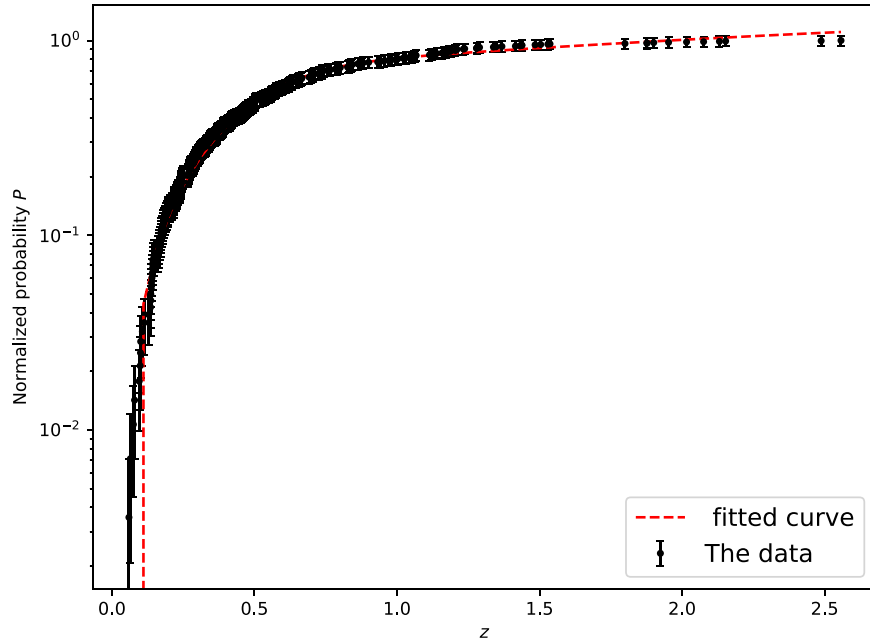


Figure 3. The normalized accumulated distributions of the observed redshift of CHIME FRBs. The red-dotted line is the fitted curve using Equation (A1).

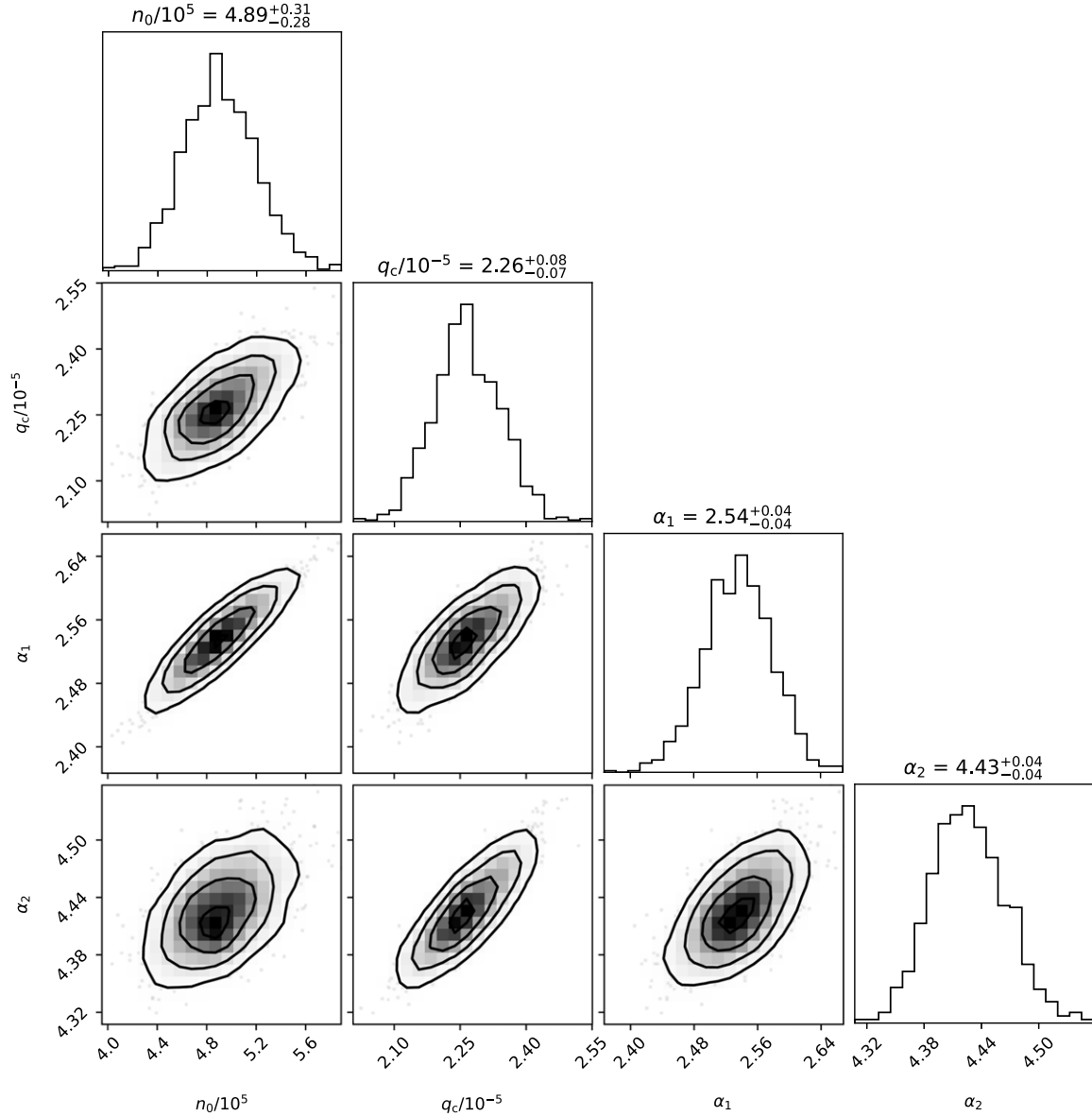


Figure 4. The posterior probability distribution of the fitting parameters derived by using the MCMC method.

based on the non-parametric approach. Of course, the results obtained here can also be used as a reference.

ORCID iDs

Can-Min Deng  <https://orcid.org/0000-0003-0471-365X>

References

- Ali-Haïmoud, Y., Kovetz, E. D., & Kamionkowski, M. 2017, *PhRvD*, **96**, 123523
- Beloborodov, A. M. 2017, *ApJL*, **843**, L26
- Beloborodov, A. M. 2020, *ApJ*, **896**, 142
- Bloom, J. S., Frail, D. A., & Sari, R. 2001, *AJ*, **121**, 2879
- Brandenberger, R., Cyr, B., & Varna Iyer, A. 2017, arXiv:1707.02397
- Cai, Y.-F., Sabancilar, E., Steer, D. A., & Vachaspati, T. 2012a, *PhRvD*, **86**, 043521
- Cai, Y.-F., Sabancilar, E., & Vachaspati, T. 2012b, *PhRvD*, **85**, 023530
- Cao, X.-F., & Yu, Y.-W. 2018, *PhRvD*, **97**, 023022
- Cao, X.-F., Yu, Y.-W., & Zhou, X. 2018, *ApJ*, **858**, 89
- CHIME/FRB Collaboration, Amiri, M., Andersen, B. C., et al. 2021, *ApJS*, **257**, 59
- Cordes, J. M., & Chatterjee, S. 2019, *ARA&A*, **57**, 417
- Cui, X.-H., Zhang, C.-M., Wang, S.-Q., et al. 2021, *MNRAS*, **500**, 3275
- Dai, Z. G. 2020, *ApJL*, **897**, L40
- Dai, Z. G., Wang, J. S., Wu, X. F., & Huang, Y. F. 2016, *ApJ*, **829**, 27
- Dai, Z. G., & Zhong, S. Q. 2020, *ApJL*, **895**, L1
- Decoene, V., Kotera, K., & Silk, J. 2021, *A&A*, **645**, A122
- Deng, C.-M. 2021, *PhRvD*, **103**, 123030
- Deng, C.-M., Cai, Y., Wu, X.-F., & Liang, E.-W. 2018, *PhRvD*, **98**, 123016

- Deng, C.-M., Wei, J.-J., & Wu, X.-F. 2019, *JHEAp*, **23**, 1
- Deng, C.-M., Zhong, S.-Q., & Dai, Z.-G. 2021, *ApJ*, **922**, 98
- Deng, W., & Zhang, B. 2014, *ApJL*, **783**, L35
- Falcke, H., & Rezzolla, L. 2014, *A&A*, **562**, A137
- Geng, J. J., & Huang, Y. F. 2015, *ApJ*, **809**, 24
- Geng, J.-J., Li, B., Li, L.-B., et al. 2020, *ApJL*, **898**, L55
- Gu, W.-M., Dong, Y.-Z., Liu, T., Ma, R., & Wang, J. 2016, *ApJL*, **823**, L28
- Gu, W.-M., Yi, T., & Liu, T. 2020, *MNRAS*, **497**, 1543
- Hashimoto, T., Goto, T., Chen, B. H., et al. 2022, *MNRAS*, **511**, 1961
- Imtiaz, B., Shi, R., & Cai, Y.-F. 2020, *EPJ*, **80**, 500
- Ioka, K., & Zhang, B. 2020, *ApJL*, **893**, L26
- Kashiyama, K., Ioka, K., & Mészáros, P. 2013, *ApJL*, **776**, L39
- Katz, J. I. 2016, *ApJ*, **826**, 226
- Kuerban, A., Huang, Y.-F., Geng, J.-J., et al. 2021, arXiv:2102.04264
- Kulkarni, S. R., Ofek, E. O., Neill, J. D., Zheng, Z., & Juric, M. 2014, *ApJ*, **797**, 70
- Kumar, P., Lu, W., & Bhattacharya, M. 2017, *MNRAS*, **468**, 2726
- Lan, H.-T., Zhao, Z.-Y., Wei, Y.-J., & Wang, F. Y. 2023, arXiv:2310.16307
- Li, L.-B., Huang, Y.-F., Geng, J.-J., & Li, B. 2018, *RAA*, **18**, 061
- Liu, T., Romero, G. E., Liu, M.-L., & Li, A. 2016, *ApJ*, **826**, 82
- Liu, X. 2018, *Ap&SS*, **363**, 242
- Lorimer, D. R., Bailes, M., McLaughlin, M. A., Narkevic, D. J., & Crawford, F. 2007, *Sci*, **318**, 777
- Lu, W., Kumar, P., & Zhang, B. 2020, *MNRAS*, **498**, 1397
- Luo, J.-W., Zhu-Ge, J.-M., & Zhang, B. 2023, *MNRAS*, **518**, 1629
- Lyu, F., Meng, Y.-Z., Tang, Z.-F., et al. 2021, *FrPhy*, **16**, 24503
- Lyubarsky, Y. 2014, *MNRAS*, **442**, L9
- Meng, M., & Deng, C. M. 2024, *A&A*, submitted
- Metzger, B. D., Berger, E., & Margalit, B. 2017, *ApJ*, **841**, 14
- Metzger, B. D., Margalit, B., & Sironi, L. 2019, *MNRAS*, **485**, 4091
- Mingarelli, C. M. F., Levin, J., & Lazio, T. J. W. 2015, *ApJL*, **814**, L20
- Palaniswamy, D., Li, Y., & Zhang, B. 2018, *ApJL*, **854**, L12
- Petroff, E., Hessels, J. W. T., & Lorimer, D. R. 2019, *A&ARv*, **27**, 4
- Planck Collaboration, Ade, P. A. R., Aghanim, N., et al. 2016, *A&A*, **594**, A13
- Popov, S. B., & Postnov, K. A. 2013, arXiv:1307.4924
- Punsly, B., & Bini, D. 2016, *MNRAS*, **459**, L41
- Qiang, D.-C., Li, S.-L., & Wei, H. 2022, *JCAP*, **2022**, 040
- Ravi, V. 2019, *NatAs*, **3**, 928
- Shin, K., Masui, K. W., Bhardwaj, M., et al. 2023, *ApJ*, **944**, 105
- Sun, H., Zhang, B., & Li, Z. 2015, *ApJ*, **812**, 33
- Totani, T. 2013, *PASJ*, **65**, L12
- Vachaspati, T. 2008, *PhRvL*, **101**, 141301
- Wadiasingh, Z., & Timokhin, A. 2019, *ApJ*, **879**, 4
- Wang, F. Y., Zhang, G. Q., Dai, Z. G., & Cheng, K. S. 2022, *NatCo*, **13**, 4382
- Wang, J.-S., Yang, Y.-P., Wu, X.-F., Dai, Z.-G., & Wang, F.-Y. 2016, *ApJL*, **822**, L7
- Wang, X.-Z., & Deng, C.-M. 2024, *EPJ*, **84**, 31
- Xiao, D., Wang, F., & Dai, Z. 2021, *SCPMA*, **64**, 249501
- Yao, J. M., Manchester, R. N., & Wang, N. 2017, *ApJ*, **835**, 29
- Ye, J., Wang, K., & Cai, Y.-F. 2017, *EPJ*, **77**, 720
- Yu, Y.-W., Cheng, K.-S., Shiu, G., & Tye, H. 2014, *JCAP*, **2014**, 040
- Zadorozhna, L. V. 2015, *AASP*, **5**, 43
- Zhang, B. 2014, *ApJL*, **780**, L21
- Zhang, B. 2016, *ApJL*, **827**, L31
- Zhang, B. 2019, *The Physics of Gamma-ray Bursts* (Cambridge: Cambridge Univ. Press)
- Zhang, B. 2020a, *Natur*, **587**, 45
- Zhang, B. 2020b, *ApJL*, **890**, L24
- Zhang, B. 2023, *RvMP*, **95**, 035005
- Zhong, S.-Q., Xie, W.-J., Deng, C.-M., et al. 2022, *ApJ*, **926**, 206
- Zhu-Ge, J.-M., Luo, J.-W., & Zhang, B. 2023, *MNRAS*, **519**, 1823